

# Numerical solution of the Stratonovich- and Ito–Euler equations: Application to the stochastic piston problem



Zhongqiang Zhang<sup>a</sup>, Xiu Yang<sup>a</sup>, Guang Lin<sup>b</sup>, George Em Karniadakis<sup>a,\*</sup>

<sup>a</sup> Division of Applied Mathematics, Brown University, Providence, RI 02912, USA

<sup>b</sup> Pacific Northwest National Laboratory, Richland, WA 99352, USA

## ARTICLE INFO

### Article history:

Received 15 May 2012

Received in revised form 25 September 2012

Accepted 5 November 2012

Available online 29 November 2012

### Keywords:

Multiplicative noise

Splitting method

Spectral expansion

Stochastic collocation

Quasi-Monte Carlo (QMC)

Shock tube

## ABSTRACT

We consider a piston with a velocity perturbed by Brownian motion moving into a straight tube filled with a perfect gas at rest. The shock generated ahead of the piston can be located by solving the one-dimensional Euler equations driven by white noise using the Stratonovich or Ito formulations. We approximate the Brownian motion with its spectral truncation and subsequently apply stochastic collocation using either sparse grid or the quasi-Monte Carlo (QMC) method. In particular, we first transform the Euler equations with an unsteady stochastic boundary into stochastic Euler equations over a fixed domain with a time-dependent stochastic source term. We then solve the transformed equations by splitting them up into two parts, i.e., a ‘deterministic part’ and a ‘stochastic part’. Numerical results verify the Stratonovich–Euler and Ito–Euler models against stochastic perturbation results, and demonstrate the efficiency of sparse grid and QMC for small and large random piston motions, respectively. The variance of shock location of the piston grows cubically in the case of white noise in contrast to colored noise reported in [1], where the variance of shock location grows quadratically with time for short times and linearly for longer times.

© 2012 Elsevier Inc. All rights reserved.

## 1. Introduction

In recent years, the polynomial chaos method and its extensions for colored noise have been advanced significantly for computational fluid dynamics problems, see e.g. [2,3]. Although there has been little attention paid on high-order numerical methods for white noise, white noise is nevertheless important in computational modeling, e.g. as a limit of colored noise when the correlation length goes to zero. An extremely small correlation length for colored noise will produce a high dimensional problem in random space and causes the so-called “curse-of-dimensionality” for high-order numerical methods which are prohibitively expensive. Unlike colored noise, white noise requires a fundamentally different calculus (see e.g. [4]) and therefore the development of new numerical methods.

Here, we revisit the stochastic piston problem in [1], which defines a testbed for numerical solvers in both random and physical space. The piston driven by time-varying random motions moves into a straight tube filled with a perfect gas at rest. Of interest is to quantify the perturbation of the shock position ahead of the piston corresponding to the random motion. For the perturbed shock position, Lin et al. [1] obtained analytical solutions for small amplitudes of noises and numerical solutions for large amplitudes of noises, with the method of stochastic perturbation analysis and polynomial chaos, respectively. A specific random motion of the piston was studied where the piston velocity was perturbed by a *correlated* random process with zero mean and exponential covariance kernel. It was concluded that the variance of the shock location grows quadrat-

\* Corresponding author. Tel. +1 401 863 1217.

E-mail address: [george\\_karniadakis@brown.edu](mailto:george_karniadakis@brown.edu) (G.E. Karniadakis).

ically with time for small time and linearly for large time by both the perturbation analysis and numerical simulations of the corresponding Euler equations. Numerical results from the Monte Carlo method and the polynomial chaos method (e.g. [5]) for the stochastic Euler equations showed good agreement with the results from the perturbation analysis.

Here we consider the case of piston velocity perturbed by *Brownian motion*, which leads to the Euler equations subject to white noise rather than the Euler equations subject to colored noise in [1]. We will use the Monte Carlo method and the recently developed stochastic collocation method for equations driven by white noise [6]. Note that the method of perturbation analysis in [1] is independent of the type of noises when they have continuous paths in the random space so that the results by the perturbation analysis can be understood in a path-wise sense. Therefore, the stochastic piston problem defined in [1] can serve as a rigorous testbed of evaluating numerical stochastic solvers. So we will use the variances from perturbation analysis as reference solutions.

Although, the Monte Carlo method is one of the popular methods for solving equations driven by white noise [7], it converges slowly as the total error of the method is dominated by the statistical error, which is proportional to  $\frac{1}{\sqrt{N}}$  with  $N$  being the number of sampling points. To avoid this slow convergence induced by the statistical error, Zhang et al. proposed in [6] a new stochastic collocation method for time-dependent equations driven by white noise in time. Stochastic collocation methods are based on high-dimensional integration quadrature rules instead of statistical methods [8–10]. While the main difficulty of the stochastic collocation method comes from the large number of random variables, in [6] we proposed a spectral expansion of the Brownian motion to reduce the number of random variables up to relatively large time for time-dependent equations so that the stochastic collocation method can be applied efficiently. Here we further extend this approach to conservation laws by adopting the quasi-Monte Carlo (QMC) method to compute up to larger time and/or for large amplitudes of noises. The QMC method is efficient and converges faster than the Monte Carlo method if relatively high dimensional integration is considered, see e.g. [11,12]; see also [13] for the application of the QMC method to elliptic equations in random porous media.

The paper is organized as follows. In Section 2, we describe the piston problem driven by random processes and review two different approaches to obtain the shock location: the perturbation analysis and the one-dimensional Euler equations. When the piston is driven by the Brownian motion, we introduce two types of Euler equations according to different interpretations of stochastic products for white noise, i.e., the Stratonovich–Euler equations and the Ito–Euler equations. In Section 3, we describe a splitting method for the Euler equations before comparing the variances from the two stochastic Euler equations with those from first-order perturbation analysis. We demonstrate that indeed the Stratonovich–Euler equations are suitable for obtaining the variances of perturbations piston locations. We apply a stochastic collocation method to solve the Stratonovich–Euler equations in the splitting-method setting. We conclude in Section 5 with a summary and comments on computational efficiency. The Appendix includes some details of the stochastic collocation method and of a model ordinary differential equation problem.

**2. Theoretical background**

Suppose that the piston velocity is perturbed by a time-dependent random process so that the piston velocity is  $u_p = U_p + v_p(t, \omega)$ , where  $\omega$  is a point in random space; see Fig. 1 for a sketch of shock tube driven by a piston perturbed with random motion. Here we write  $v_p(t, \omega) = \epsilon U_p V(t, \omega)$  and denote the stochastic process  $V(t, \omega)$  as  $V(t)$  for brevity.

When  $\epsilon = 0$ , i.e., no perturbation is imposed on the piston, the piston moves into the tube with a constant velocity  $U_p$ , the shock speed  $S$  (and thus the shock location) can be determined analytically, see [1,14]. When  $\epsilon$  is very small, one can determine the perturbation process of the shock location using the first-order perturbation analysis [1], that is:

$$z(t) = \epsilon U_p q S^q \sum_{n=0}^{\infty} (-r)^n \int_0^t V(\alpha \beta^n t_1) dt_1, \tag{2.1}$$

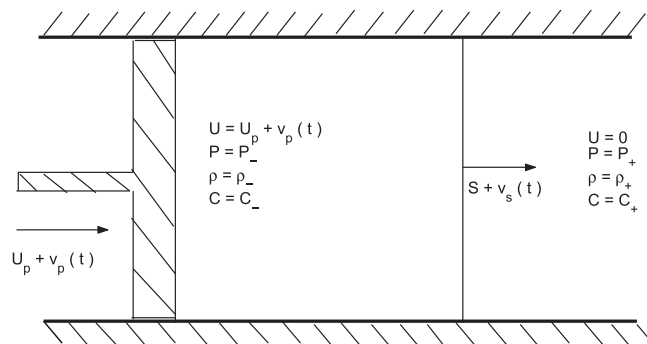


Fig. 1. A sketch of piston-driven shock tube with random piston motion.

where  $z(t) + tS$  is the shock location induced by the random motion of piston,

$$S' = \frac{\gamma + 1}{4} \frac{S}{S - \frac{\gamma+1}{4}U_p},$$

$$q = \frac{2}{1+k}, \quad r = \frac{1-k}{1+k}, \quad k = C_- \frac{S + S'U_p}{1 + \gamma S U_p},$$

$$\alpha = \frac{C_- + U_p - S}{C_-}, \quad \beta = \frac{C_- + U_p - S}{C_- + S - U_p}.$$

Here  $\gamma$  is the ratio of the specific heats and  $C_-$  the sound speed behind the shock when the piston is unperturbed. The first two moments of the perturbation process  $z(t)$  are

$$\mathbb{E}[z(t)] = 0,$$

$$\mathbb{E}[z^2(t)] = (\epsilon U_p q S')^2 \mathbb{E} \left[ \left( \sum_{n=0}^{\infty} (-r)^n \int_0^t V(\alpha \beta^n t_1, \cdot) dt_1 \right)^2 \right].$$

We note that the perturbation analysis in [1] is independent of the perturbation process whenever the process is continuous such that the analysis can be understood in a path-wise way. By taking  $V(t, \omega)$  as the Brownian motion  $W(t)$  (omitting  $\omega$ ), we then have

$$\mathbb{E}[z^2(t)] = (\epsilon U_p q S')^2 \mathbb{E} \left[ \left( \sum_{n=0}^{\infty} (-r)^n \int_0^t W(\alpha \beta^n t_1) dt_1 \right)^2 \right] = (\epsilon U_p q S')^2 \mathbb{E} \left[ \left( \sum_{n=0}^{\infty} (-r)^n \int_0^t \sqrt{\alpha \beta^n} W(t_1) dt_1 \right)^2 \right]$$

$$= (\epsilon U_p q S')^2 \left( \sum_{n=0}^{\infty} (-r)^n \sqrt{\alpha \beta^n} \right)^2 \mathbb{E} \left[ \left( \int_0^t W(t_1) dt_1 \right)^2 \right] = \frac{\alpha t^3}{3} (\epsilon U_p q S')^2 \frac{1}{(1 + r\beta^{\frac{1}{2}})^2}, \tag{2.2}$$

where we use the scaling property of Brownian motion ( $W(\alpha \beta^n t_1) = \sqrt{\alpha \beta^n} W(t_1)$ ) and  $\int_0^t W(t_1) dt_1$  is a Gaussian process with zero mean and variance  $\frac{t^3}{3}$ .

### 2.1. Stochastic Euler equations

The stochastic piston problem can be modeled by the following Euler equations with unsteady stochastic boundary:

$$\frac{\partial}{\partial t} \mathbf{U} + \frac{\partial}{\partial x} (f(\mathbf{U})) = 0, \tag{2.3}$$

where  $\mathbf{U} = \begin{pmatrix} \rho \\ \rho u \\ E \end{pmatrix}$ ,  $f(\mathbf{U}) = \begin{pmatrix} \rho u \\ \rho u^2 + P \\ u(P + E) \end{pmatrix}$ ,  $\rho$  is density,  $u$  is velocity,  $E$  is total energy, and  $P$  is pressure given by  $(\gamma - 1)(E - \frac{1}{2}\rho u^2)$  and  $\gamma = 1.4$ . The initial and boundary conditions are given by

$$u(x, 0) = 0, \quad P(x, 0) = P_+, \quad \rho(x, 0) = \rho_+, \quad x > X_p(t),$$

$$P(X_p(t), 0) = P_-, \quad \rho(X_p(t), 0) = \rho_-$$

and

$$u(X_p(t), t) = \frac{\partial}{\partial t} X_p(t) = u_p(t), \quad t > 0,$$

where  $X_p(t)$  is the position of the piston, and  $u_p(t)$  is the velocity of the piston.

This problem is a moving boundary problem and can be transformed to a fixed boundary problem by defining a new coordinate  $(y, \tau)$  from  $(x, t)$  via the following transform:

$$y = x - \int_0^\tau u_p(\tau_1, \omega) d\tau_1, \quad \tau = t. \tag{2.4}$$

Defining  $v = u - u_p$ , we then have the following Euler equations with a source term [1]:

$$\frac{\partial}{\partial \tau} \mathbf{V} + \frac{\partial}{\partial y} (f(\mathbf{V})) = \mathbf{g}(\mathbf{V}) \frac{\partial u_p}{\partial \tau}, \tag{2.5}$$

where  $\mathbf{V} = \begin{pmatrix} \rho \\ \rho v \\ \tilde{E} \end{pmatrix}$ ,  $\tilde{E} = \frac{P}{\gamma-1} + \frac{1}{2}\rho v^2$  and  $\mathbf{g}(\mathbf{V}) = \begin{pmatrix} 0 \\ -\rho \\ -\rho v \end{pmatrix}$ . The initial and boundary conditions are given by

$$\begin{aligned} v(y, 0) &= -U_p, \quad P(y, 0) = P_+, \quad \rho(y, 0) = \rho_+, \quad y > 0, \\ P(0, 0) &= P_-, \quad \rho(0, 0) = \rho_- \end{aligned} \quad (2.6)$$

and

$$v(0, \tau) = 0, \quad \tau \geq 0.$$

Our goal here is to compute the variance of the shock location perturbation  $z(\tau)$ . The perturbation of the shock location is  $z(\tau) = X_s(\tau) - \tau S = X_s(\tau) - tS$ , where  $X_s(\tau) = Y_s(\tau) + \int_0^\tau u_p(t_1) dt_1$  is the shock location while  $Y_s(\tau)$  is the shock location under the new coordinate  $(y, \tau)$ .

If we take  $u_p(t) = U_p(1 + \epsilon W(t))$ , where  $W(t)$  is a scalar Brownian motion, we are led to the following Euler equations

$$\frac{\partial}{\partial \tau} \mathbf{V} + \frac{\partial}{\partial y} (f(\mathbf{V})) = \epsilon U_p g(\mathbf{V}) * \dot{W}, \quad (2.7)$$

where ‘\*’ denotes two different products as follows:

(1) Stratonovich–Euler equations

$$\frac{\partial}{\partial \tau} \mathbf{V} + \frac{\partial}{\partial y} (f(\mathbf{V})) = \epsilon U_p g(\mathbf{V}) \circ \dot{W}, \quad (2.8)$$

where ‘ $\circ$ ’ is the Stratonovich product, or

(2) Ito–Euler equations

$$\frac{\partial}{\partial \tau} \mathbf{V} + \frac{\partial}{\partial y} (f(\mathbf{V})) = \epsilon U_p g(\mathbf{V}) \cdot \dot{W}, \quad (2.9)$$

where ‘ $\cdot$ ’ is the Ito product. The initial and boundary conditions are imposed as above. The meaning of ‘ $\circ$ ’ will be explained in Section 3.2 and that of ‘ $\cdot$ ’ in Section 3.3.

We will verify these two models (2.8) and (2.9) by solving them numerically with a splitting method in the next section.

### 3. Verification of the Stratonovich- and Ito–Euler equations

In the previous section, we introduced two approaches to obtain the variances of the shock location. Here, we verify the correctness of the stochastic Euler equations by comparing the variances of the shock location obtained by two approaches, i.e., the first-order perturbation analysis and the numerical solution of the stochastic Euler equations, up to time  $T = 5$ .

For numerical simulations, we consider the piston velocity  $U_p = 1.25$ , where the Mach number of the shock is  $M = 2$  and  $\gamma = 1.4$ . We normalize all velocities with  $C_+$ , the sound speed ahead of the shock, i.e.  $C_+ = 1$ . Then, the initial conditions are given through the unperturbed relations of states variables [1] as follows:

$$P_+ = 4.5, \quad P_- = 1.0, \quad \rho_+ = 3.73, \quad \rho_- = 1.4.$$

#### 3.1. A splitting method for stochastic Euler equations

We use a source-term (noise-term) splitting method proposed in [15] for a scalar conservation law with time-dependent white noise source term. Holden and Risebro [15] considered a Cauchy problem on the whole line with multiplicative white noise in Ito’s sense:  $\frac{\partial}{\partial t} u + \frac{\partial}{\partial x} f(u) = g(u) \dot{W}(t)$  with deterministic essentially bounded initial condition where  $f, g$  are both Lipschitz, and  $g$  has bounded support. They proved the *almost-sure-convergence* of this splitting method to a weak solution of the Cauchy problem assuming initial condition having bounded support and finitely many extrema while provided no convergence rate.

Here we extend this splitting method to the system (2.7). Specifically, given the solution at  $\tau_n$ ,  $\mathbf{V}^n$ , to obtain the solution at  $\tau_{n+1}$ , we first solve, on the small time interval  $[\tau_n, \tau_{n+1})$ ,

$$\frac{\partial}{\partial \tau} \mathbf{V}^{(1)} + \frac{\partial}{\partial y} (f(\mathbf{V}^{(1)})) = 0, \quad (3.1)$$

with the boundary conditions (2.6) and initial condition  $\mathbf{V}^{(1)}(\tau_n) = \mathbf{V}^n$ ; then we solve the following Cauchy problem, again on  $[\tau_n, \tau_{n+1})$ ,

$$\frac{\partial}{\partial \tau} \mathbf{V}^{(2)} = \epsilon U_p g(\mathbf{V}^{(2)}) * \dot{W}, \quad (3.2)$$

with the initial condition  $\mathbf{V}^{(2)}(\tau_n) = \mathbf{V}^{(1)}(\tau_{n+1})$ . Then the solution at time  $\tau_{n+1}$ ,  $\mathbf{V}^{n+1}$ , is set as  $\mathbf{V}^{(2)}(\tau_{n+1})$  (subject to the error from the splitting). If we denote by  $S(\tau, \tau_n)$  the operator which takes  $\mathbf{V}(\tau_n)$  as initial condition at  $\tau_n$  to the weak solution of (3.1) and by  $R(\tau, \tau_n)$  the operator which takes the initial condition at time  $\tau_n$  to the solution of the stochastic differential equation (3.2). Then the approximate solution at  $\tau_{n+1}$  is defined by  $\mathbf{V}^{n+1} = R(\tau_{n+1}, \tau_n)S(\tau_{n+1}, \tau_n)\mathbf{V}^n$ . Thus we define a sequence of approximate solution,  $\{\mathbf{V}^n\}$ , to (2.7) at time  $\{\tau_n\}$ .

The application of splitting technique requires numerical methods for (3.1) and (3.2). The splitting scheme allows us to deploy efficient existing methods to solve them separately. To solve (3.1), we use a fifth-order WENO scheme in physical space and second-order strong-property-preserving (SPP) Runge–Kutta in time [16]. In solving (3.2), we will employ two different methods: the Monte Carlo method and the stochastic collocation method developed in [6]. We employ 1000 points for the fifth-order WENO scheme over the interval  $[0, 5]$  and the time step size  $d\tau = 0.0005$  so that the error from time discretization is negligible. As we mentioned before, our goal is to compute the variance of the perturbed shock location. Since there is always only one shock, we obtain  $Y_s(\tau)$  by finding the biggest jump of pressure, where the error is of order  $O(dx)$  ( $dx$  is the mesh size in physical space).

### 3.2. Stratonovich–Euler equations versus first-order perturbation analysis

We first compare the results obtained by solving the Stratonovich–Euler equations with the Monte Carlo method and those obtained from first-order perturbation analysis.

To solve the Stratonovich–Euler equation (2.8) with the splitting method, we need to solve (3.2) as follows. By the definition of the Stratonovich integral, we have that, for a square-integrable stochastic process  $h(t)$ ,

$$\int_0^T h(t) \circ dW = \lim_{n \rightarrow \infty} h(t_{n+1/2}) \Delta W_n,$$

where  $t_{n+1/2} = \frac{t_{n+1} + t_n}{2}$  and  $\Delta W_n = W(t_{n+1}) - W(t_n)$ . The limit is understood in the mean-square sense [4]. Thus, we will solve Eq. (3.2) by the following Crank–Nicolson scheme

$$\mathbf{V}^{(2)}(\tau_{n+1}) = \mathbf{V}^{(2)}(\tau_n) + \epsilon U_p g(\mathbf{V}^{(2)}(\tau_{n+1/2})) \Delta W_n. \tag{3.3}$$

In our simulation, the values of function  $g(\mathbf{V}^{(2)}(\tau))$  at  $\tau_{n+1/2}$  are approximated by the average values  $\frac{g(\mathbf{V}^{(2)}(\tau_n)) + g(\mathbf{V}^{(2)}(\tau_{n+1}))}{2}$ . Note that for the specific form of  $g$ , we do not have to invert the resulting matrix in (3.3).

Fig. 2 verifies that the Stratonovich–Euler equation (2.8) can capture the variances of shock location for the stochastic piston problem driven by Brownian motion. Here we employ 10,000 realizations so that the statistical error can be neglected for noises with amplitude no less than 0.05. We also note that for noises with amplitude less than 0.05, the error of the adopted methods is dominated by the statistical error from the Monte Carlo method and also the space discretization error from WENO. Fig. 2 presents the variances obtained by the Monte Carlo method (3.1)–(3.3) and those from variances estimates by the first-order perturbation analysis (2.2). We observe the agreement between the results from the Monte Carlo method and the perturbation analysis within small time and for small noises. Fig. 2(a) shows the results for small noises, i.e.,  $\epsilon \sim O(10^{-2})$  while Fig. 2(b) for large noises, i.e.,  $\epsilon \sim O(10^{-1})$ . The difference between the variances from the Monte Carlo method and the first-order perturbation analysis (2.2) is at most 12 – 13% of the variances (2.2), up to time  $T = 5$ , for all cases except for the case  $\epsilon = 0.5$ ; for the latter, the difference between the variances is at most 19.3% of the variance (2.2). However, for small time ( $t < 1$ ) the variances by Monte Carlo and perturbation analysis agree well, while they deviate much after  $t = 2$ . This effect can be explained as follows. For  $t < 1$ , the variance of the driving process (Brownian motion) has small value ( $\sqrt{t}$ ) corresponding to a weak perturbation; while at later time it has larger value increasing substantially the perturbation. (We remind the reader that the perturbation process in [1] has unit variance.)

### 3.3. Stratonovich–Euler equations versus Ito–Euler equations

For the Ito–Euler equation (2.9), we solve (3.2) by the forward Euler scheme

$$\mathbf{V}^{(2)}(\tau_{n+1}) = \mathbf{V}^{(2)}(\tau_n) + \epsilon U_p g(\mathbf{V}^{(2)}(\tau_n)) \Delta W_n. \tag{3.4}$$

Recall that the Ito integral is defined as, see e.g. [4],

$$\int_0^T h(t) \cdot dW = \lim_{n \rightarrow \infty} h(t_n) \Delta W_n.$$

Next we compare the numerical results for the Stratonovich–Euler equations and the Ito–Euler ones using the above discretization in time. We observe from Fig. 3 that for both small and large noises, these two types of equations have almost the same variances for the perturbed shock location  $\mathbb{E}[z^2(t)]$  up to time  $T = 5$ . Actually, the difference of variances by the Stratonovich–Euler and Ito–Euler equations for  $\epsilon \leq 0.2$  is less than  $10^{-3}$  up to time  $t = 5$  which lies within the discretization errors. For  $\epsilon = 0.5$ , we present in Table 1 the difference of variances for these two approaches using the same sequence of Monte Carlo points. The Stratonovich–Euler equations exhibits larger variances in large time but the difference from those

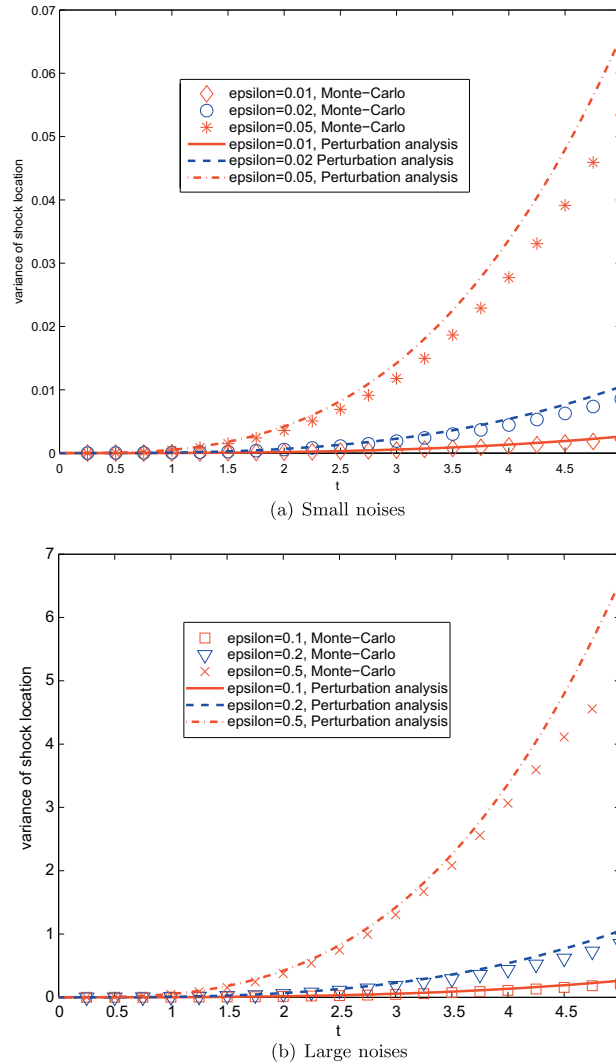


**Fig. 2.** Comparison between the results from first-order perturbation analysis (2.2) and solving the Stratonovich–Euler equation (2.8) by the splitting method (3.1)–(3.3).

by the Ito–Euler equations is less than 10% of the variances by Ito–Euler equations. We then conclude that the Stratonovich–Euler equations are a suitable model for the piston problem driven by Brownian motion and we will consider only this approach hereafter.

**4. The stochastic collocation method**

Next we test the stochastic collocation method versus the Monte Carlo method for the Stratonovich–Euler equation (2.8). To solve the Stratonovich–Euler equation (2.8), we again use the splitting method (3.1) and (3.2). In (3.2), we adopt the stochastic collocation method [6], where we first introduce a spectral approximation for the Brownian motions and subsequently apply the sparse grid method. Specifically, we first approximate Brownian motion with its spectral approximation, using  $K$  multi-elements:

$$W^{(n,K)}(\tau) = \sum_{k=0}^{K-1} \sum_{i=1}^n \int_0^\tau \chi_{[t_k, t_{k+1})}(s) m_i^{(k)}(s) ds \zeta_i^{(k)}, \tau \in [0, T],$$

where  $0 = t_0 < t_1 < \dots < t_K = T$ ,  $\chi_{[t_k, t_{k+1})}(\tau)$  is the indicator function of the interval  $[t_k, t_{k+1})$ ,  $\{m_i^{(k)}\}_{i=1}^\infty$  is a complete orthonormal basis in  $L^2([t_k, t_{k+1}])$ , and  $\zeta_i^{(k)}$  are mutually independent standard Gaussian random variables (with zero mean and variance one). Hence, we obtain the following partial differential equation with smooth inputs:

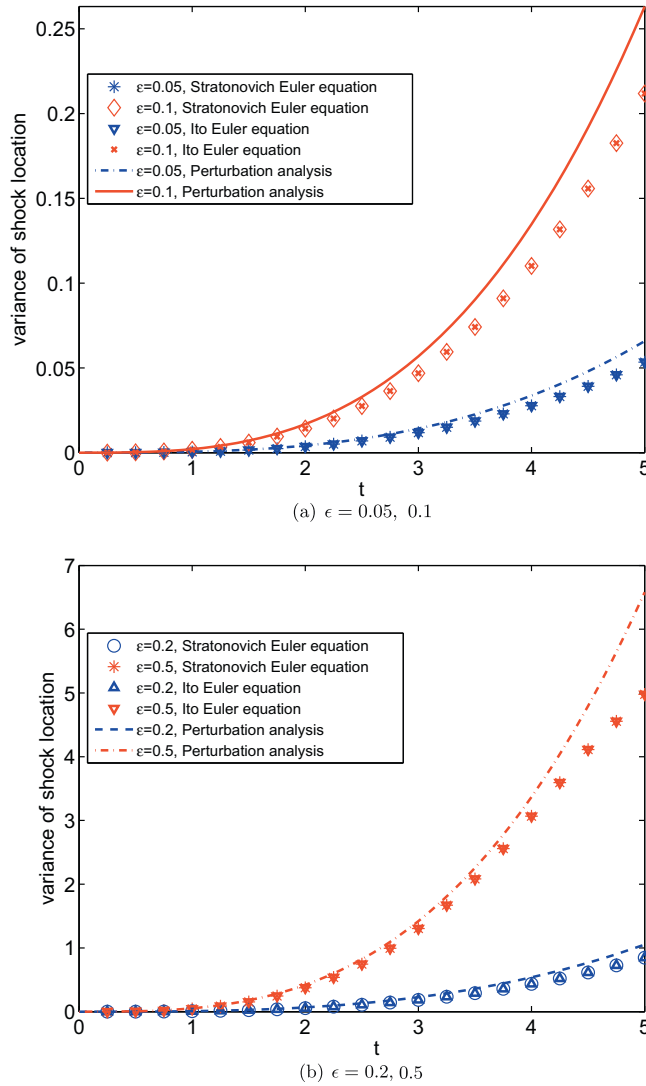


Fig. 3. Comparison between solving Stratonovich–Euler equation (2.8) and Ito–Euler equation (2.9) by the splitting method (3.1) and (3.2).

Table 1

The difference of variances of shock location by Stratonovich–Euler and Ito–Euler equations for  $\epsilon = 0.5$ .

$t$	1.0	2.0	3.0	4.0	5.0
	0.0007	0.0129	0.0742	0.2353	0.2421

$$\frac{\partial}{\partial \tau} \mathbf{V}^{(2)} = \epsilon U_p \mathbf{g}(\mathbf{V}^{(2)}) \sum_{k=0}^{K-1} \sum_{i=1}^n \chi_{[t_k, t_{k+1})}(\tau) m_i^{(k)}(\tau) \zeta_i^{(k)}. \tag{4.1}$$

In (4.1) we apply the stochastic collocation method [8–10] for smooth noises; see Appendix A for a brief review on the stochastic collocation method for white noise and [6] for more details. The stochastic collocation method we adopt here is the sparse grid of Smolyak type based on 1D Gaussian–Hermite quadrature; we refer to [17] for implementation details.

The first issue we have for the piston problem here is the discontinuity of the solution to (2.8), where the condition for spectral approximation to work may be invalid [18,6]. In practice, we solve the problem with the WENO scheme, which smears the shock somewhat, and thus we have higher regularity than that of the original problem. A second issue is that the use of the stochastic collocation method (Smolyak sparse grid) with Gaussian quadrature may not exhibit fast convergence because of the low regularity. Thus, we use  $n = 1$  or  $2$  with large  $K$  (small time step in  $W^{(n,K)}$ ) instead of large  $n$  with small  $K$ . This choice of  $n$  is verified with control tests with  $n = 3, 4$  for different  $K$ , where the numerical results show large

deviations from those of Monte Carlo method with high oscillations. We choose a low sparse grid level (i.e. two) to be consistent with the ‘available regularity’ (numerical tests with high sparse grid level show an instability). The third issue is the so-called “curse-of-dimensionality”. In practice, when the number of random variables,  $Kn$ , increases, the Smolyak sparse grid method will not work well and will be replaced by the QMC method.

Here we adopt a uniform partition of the time interval  $[0, T]$ , that is  $t_k = (k - 1)\Delta$ ,  $k = 1, \dots, K$ . The complete orthonormal basis we employ in  $L^2([t_k, t_{k+1}])$  is the cosine basis

$$m_1^{(k)}(t) = \frac{1}{\sqrt{\Delta}}, \quad m_i^{(k)}(t) = \sqrt{\frac{2}{\Delta}} \cos\left(\frac{(i-1)\pi}{\Delta}(t - t_k)\right), \quad i \geq 2.$$

Fig. 4 compares the numerical results from the Monte Carlo method (3.1)–(3.3) and the stochastic collocation method for (3.1) and (4.1) with both small and large noises. For each  $\epsilon$ , we use different  $\Delta$  (the length of the uniform partition of time interval  $[0, T]$ ), i.e. different size of elements  $K$ . We note that all the numerical solutions obtained by the stochastic collocation method agree with those from the Monte Carlo method (3.1)–(3.3) within small time. Here we do not observe convergence in  $n$ , recalling that such convergence requires smoothness in random space [6].

We note that smaller  $\Delta$  and larger  $n$  may lead to a larger number of random variables and thus the break down of the sparse grid method [10]. So we first test the cases of small  $\Delta$  such that we can apply the sparse grid method. Fig. 4 shows that a low level sparse grid method works well for the piston problem with small perturbations. We note that our sparse grid level is two and thus the number of collocation points is  $2n\frac{T}{\Delta} + 1$ .

When  $n = 1$ , we observe in Fig. 4 good agreement of the results by the stochastic collocation method and the Monte Carlo method in small time ( $t \leq 2$ ). Notice that when  $n = 1$ , (4.1) is the classical Wong–Zakai approximation [19]

$$\frac{\partial}{\partial \tau} \mathbf{V}^{(2)} = \mathbf{g}(\mathbf{V}^{(2)}) \frac{1}{\sqrt{\Delta}} \sum_{k=0}^{K-1} \chi_{[t_k, t_{k+1})}(\tau) \xi_1^{(k)}. \tag{4.2}$$

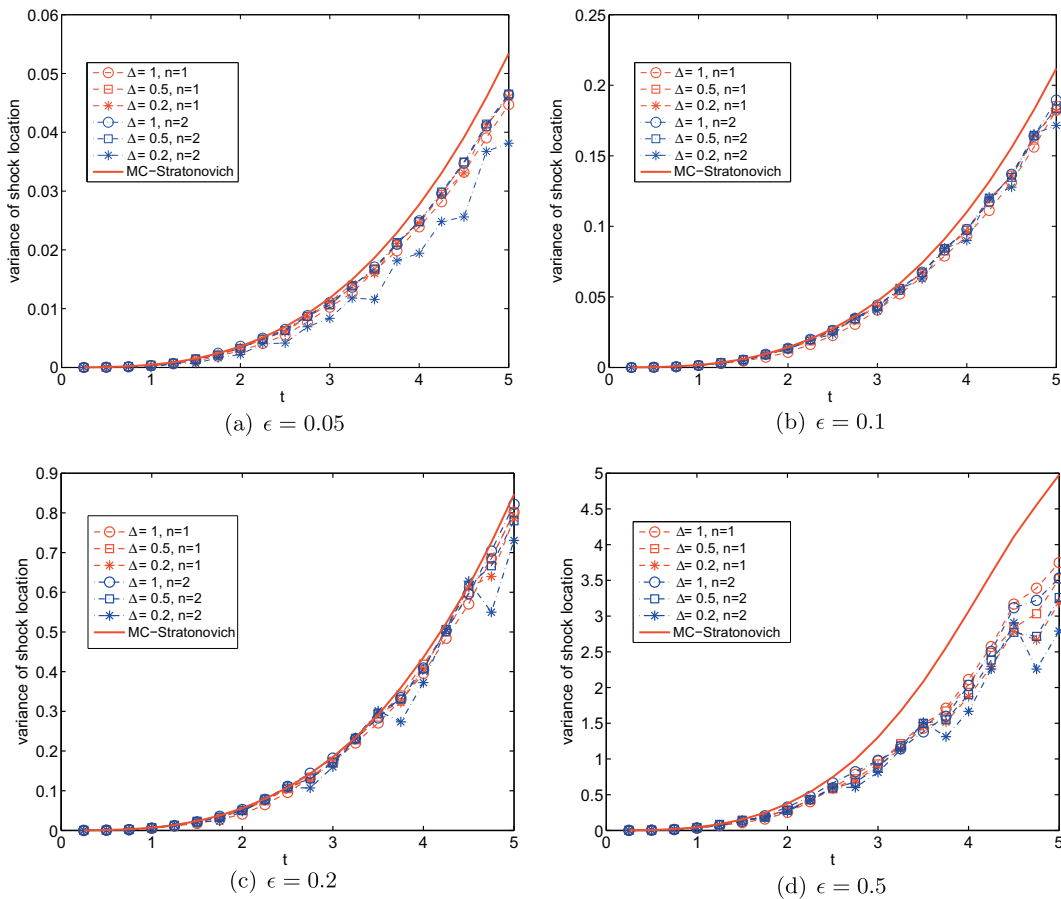


Fig. 4. Comparison between numerical results from Stratonovich–Euler equation (2.8) using the direct Monte Carlo method (3.1) and (3.3) and the stochastic collocation method (4.1). The sparse grid level is 2 and  $\Delta$  is the size of element in time in the stochastic collocation method.

However, for  $n = 2$ , there are some disagreements between the results. In Fig. 4(a) and 4(c), the results of the case  $n = 2$  and  $\Delta = 0.2$  (note that we have  $nK = 50$  random variables) underestimate those results from the Monte Carlo method and the stochastic collocation method with a smaller number of random variables ( $n = 1$ ). The larger number of random variables ( $n = 2$  here) does not result in convergence since we do not have a smooth solution as we mention above.

For the case with large perturbation,  $\epsilon = 0.5$ , we require smaller  $\Delta$  and thus more random variables. This is why we observe the disagreement in Fig. 4(d). For all cases in Fig. 4, we observe a deviation of numerical results by stochastic collocation methods from those of Monte Carlo method over large time. Similar effects arise in the application of spectral methods in random space, e.g., in Wiener chaos methods. The interested reader may refer to [20] for a discussion of this effect.

To adapt to the high dimensionality (large number of random variables), we employ the QMC method instead of sparse grid methods. We consider two popular QMC sequences: one is a scrambled Halton with the method RR2 proposed in [21]; and the other is a scrambled Sobol sequence suggested in [22]. Both sequences lie in hypercube and thus an inverse transformation is adopted to generate sequences in the entire space based on these two sequences. In Fig. 5, we test the large noise case, i.e.  $\epsilon = 0.5$ . Both Halton and Sobol sequences work if a moderately large sample of the sequences is adopted. For 1000 sample points, variances from both sequences are closer to those from Monte Carlo method (3.1)–(3.3) than those from 500 sample points of both sequences.

### 5. Summary

We simulated a stochastic piston problem by time-varying Brownian motions of a piston moving inside an adiabatic tube of constant area, which is governed by the Euler equations driven by white noise. By splitting the Euler equations into two

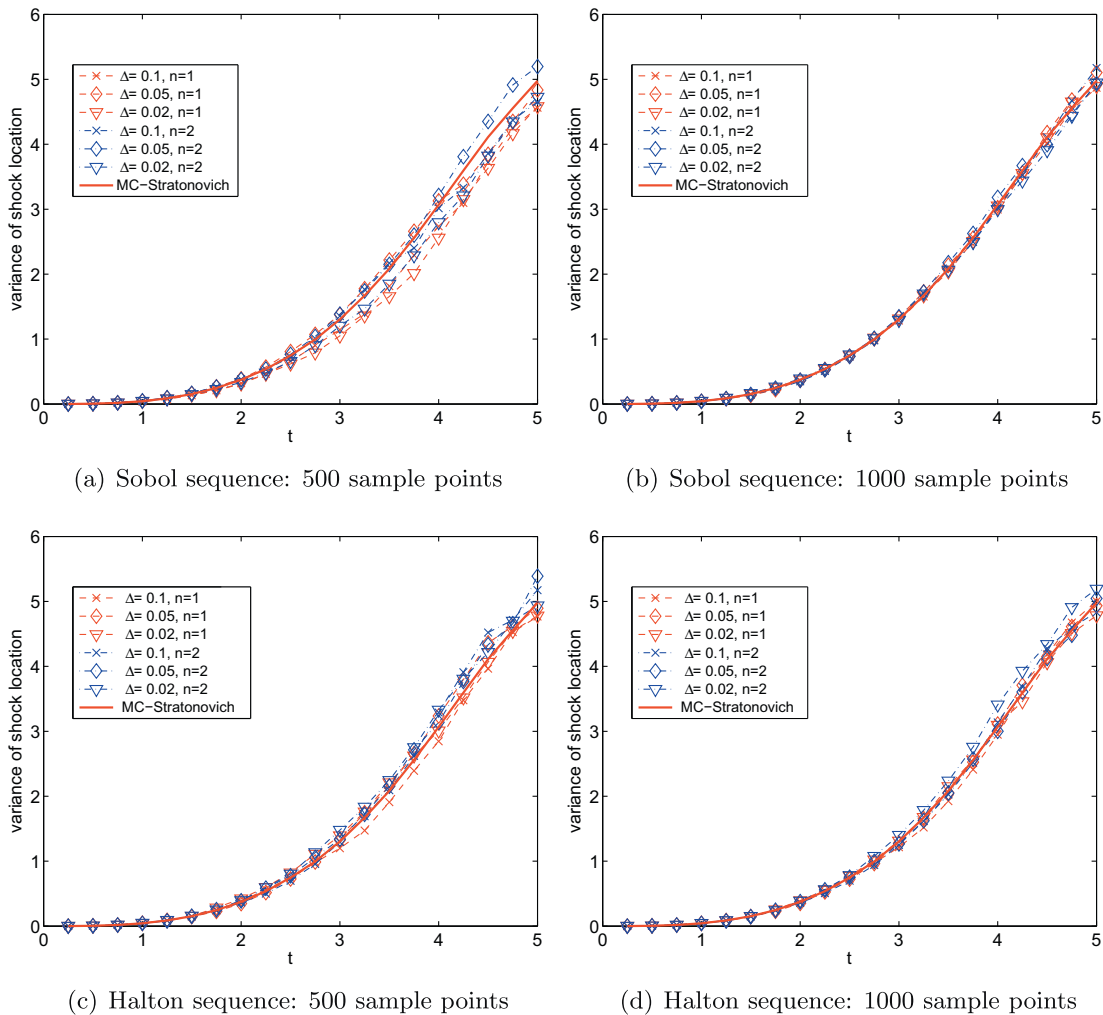
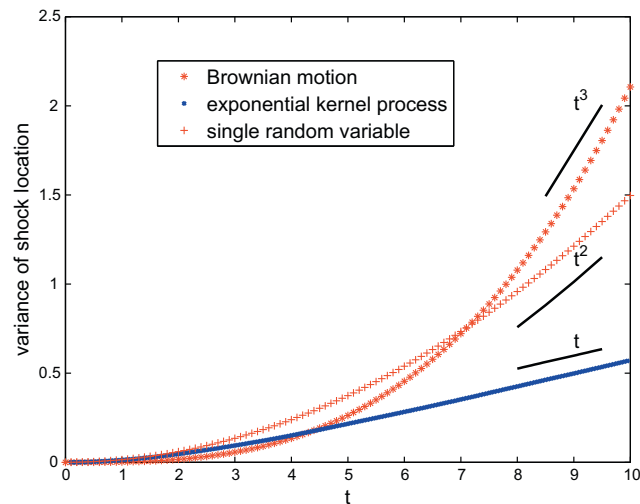


Fig. 5. Comparison between numerical results from Stratonovich–Euler equation (2.8) using direct Monte Carlo method (3.1)–(3.3) and the QMC method for (4.1) with a large noise:  $\epsilon = 0.5$ .



**Fig. 6.** Comparison among variances of shock positions induced by three different Gaussian noises: Brownian motion, random process with zero mean and exponential covariance kernel  $\exp(-|t_1 - t_2|)$  and standard Gaussian random variable. The noise amplitude is  $\epsilon = 0.1$ .

parts – a ‘deterministic part’ and a ‘stochastic part’ – we solved the ‘stochastic part’ by the Monte Carlo method and the stochastic collocation method. The numerical results show that the variances of the shock location grow cubically with time, which are significantly different from those from colored noise driven piston. In Fig. 6 we compare the variances of shock positions induced by three different Gaussian noises: Brownian motion, random process with zero mean and exponential covariance kernel  $\exp(-|t_1 - t_2|)$ , and standard Gaussian random variable, where the noise amplitude is  $\epsilon = 0.1$ . The results are obtained via the stochastic perturbation analysis. The case of Brownian motion induces smaller values of variances than the other two cases for short times and greater values of variances for longer times. We note that the effects of different Gaussian processes are similar to a first-order stochastic differential equation responding to different Gaussian processes. The shock location depends on the time integration of the underlying Gaussian processes as the solution to stochastic differential equation does; see Appendix B for details.

Firstly, we solved the ‘stochastic part’ using the Monte Carlo method by the definition of Stratonovich integral and verified the Stratonovich–Euler equations by the first-order perturbation analysis presented in [1]. Secondly, we solved the Stratonovich–Euler equations by solving the ‘stochastic part’ with the stochastic collocation method using a multi-element spectral approximation of the Brownian motion. Finally, we tested two types of QMC sequences for the ‘stochastic part’ using a multi-element spectral approximation of the Brownian motion when the noise is large. The stochastic collocation and QMC methods are superior to the Monte Carlo method in the sense that they can achieve faster convergence than the classic Monte Carlo method.

The low accuracy of the stochastic collocation method, especially for long times, is caused by the discontinuity of the solution. Due to the deterministic solver, we have that the accuracy for the numerical shock location is only first-order in the spatial step size, i.e.,  $O(dx)$ . For small noises, we had agreement between the results from the Euler solver and those from perturbation analysis. However, for large noises, we need small time-interval  $\Delta$  for the stochastic collocation method to converge. As smaller time-interval  $\Delta$  leads to larger number of random variables, we adopted the QMC method which led to accurate solutions.

With regards to computational efficiency, the stochastic collocation method is more efficient than Monte Carlo simulation when a small number of random variables are involved, where the number of collocation points is far less than Monte Carlo sampling points. As time becomes larger, we introduce more random variables and thus we need to employ the more efficient QMC method. In other applications involving long-time integration, it may be possible to use all three different ways of sampling, i.e., starting with sparse grid for early time, continuing with the QMC for moderate time and even switching to the Monte Carlo method for long time.

## Acknowledgments

GEK would like to acknowledge support by MURI/AFOSR and NSF. GEK and GL also acknowledge joint support by the Applied Mathematics program of the US DOE Office of Advanced Scientific Computing Research. Computations were performed using the computational resources of the National Energy Research Scientific Computing Center at Lawrence Berkeley National Laboratory and the William R. Wiley Environmental Molecular Sciences Laboratory (EMSL). EMSL is a DOE national scientific user facility located at PNNL. The Pacific Northwest National Laboratory is operated by Battelle for the US Department of Energy under Contract DE-AC05-76RL01830.

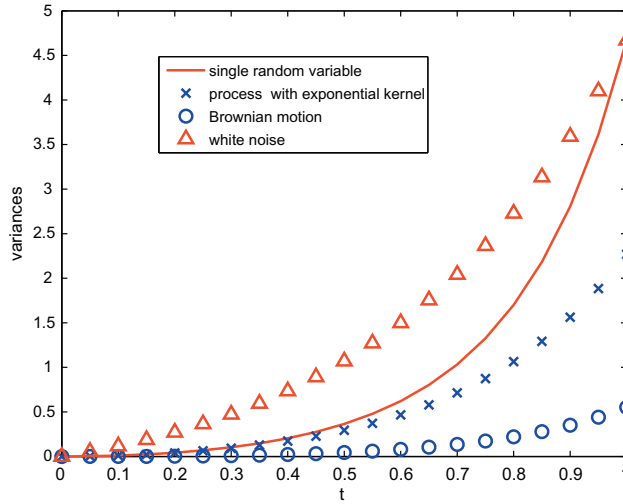


Fig. 7. Comparison of variances of the solutions for four models of  $k(t)$  up to time  $t = 1 : A = 1$ .

**Appendix A. A brief review of the stochastic collocation method for white-noise driven equations**

We describe briefly the stochastic collocation method for stochastic ordinary equations in the following form

$$dX = b(t, X)dt + \sigma(t, X) \circ dW(t), \quad X(0) = X_0, \tag{A.1}$$

where  $W(t)$  is the Brownian motion, ‘ $\circ$ ’ indicates the Stratonovich integral. A popular approach for Eq. (A.1) is to approximate the Brownian motion with a smoother process (than the Brownian motion), which is called Wong–Zakai approximation (see Wong and Zakai [19,23]). In [6], we proposed the following multi-element spectral approximation of the Brownian motion to solve Eq. (A.1):

$$W^{(n,K)}(t) = \sum_{k=0}^{K-1} \sum_{i=1}^n \int_0^t \chi_{[t_k, t_{k+1})}(s) m_i^{(k)}(s) d\xi_i^{(k)}, \quad t \in [0, T],$$

where  $0 = t_0 < t_1 < \dots < t_K = T$ ,  $\chi_{[t_k, t_{k+1})}(t)$  is the indicator function of the interval  $[t_k, t_{k+1})$  and  $\xi_i^{(k)}$  are mutually independent standard Gaussian random variables. Here  $\{m_i^{(k)}\}_{i=1}^\infty$  is a complete orthonormal basis in  $L^2([t_k, t_{k+1}])$ , e.g. the cosine basis

$$m_1^{(k)}(t) = \frac{1}{\sqrt{t_{k+1} - t_k}}, \quad m_i^{(k)}(t) = \sqrt{\frac{2}{t_{k+1} - t_k}} \cos\left(\frac{(i-1)\pi}{t_{k+1} - t_k}(t - t_k)\right), \quad i \geq 2.$$

The multi-element spectral approximation of Wong–Zakai types leads to the following ordinary differential equation with smooth inputs:

$$d\tilde{X} = b(t, \tilde{X})dt + \sigma(t, \tilde{X}) \sum_{i=1}^n \sum_{k=1}^K \chi_{[t_{k-1}, t_k)}(t) m_i^{(k)}(t) \xi_i^{(k)} dt, \quad \tilde{X}(0) = X_0. \tag{A.2}$$

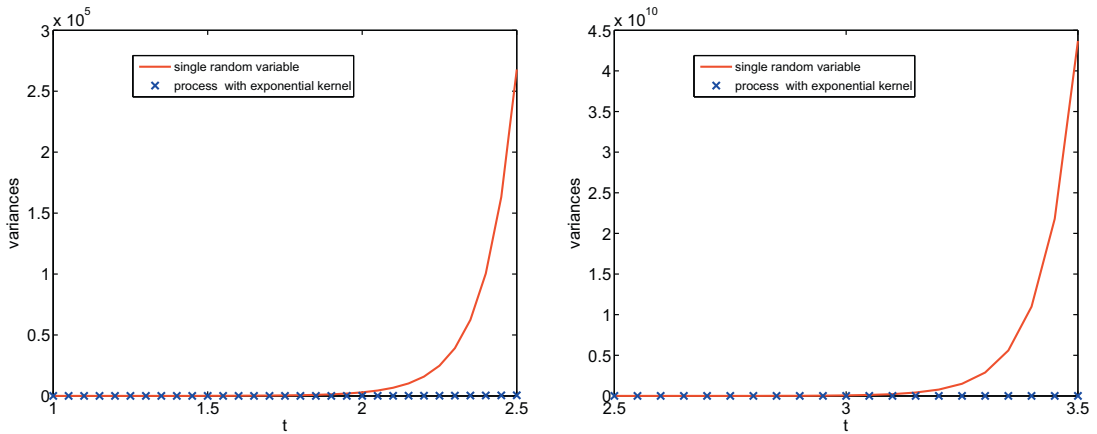
The convergence of this approximation is guaranteed by Sussmann’s Theorems [18]. Compared to other popular methods for solving (A.1) which involves only the increments of Brownian motion, it often suffices to use just a few random variables at every step of the spectral approximation of Brownian motion[6]. This effect allows us to relax the restrictions on the dimensionality quite dramatically.

To solve (A.2), we propose non-statistical stochastic collocation methods [8–10] for (A.2) so that we avoid the slow convergence of the Monte Carlo method whose error is usually dominated by the statistical error, which is proportional to  $\frac{1}{\sqrt{N}}$  with  $N$  being the number of sampling points. If  $T$  is not too large, we showed that the proposed approach has spectral convergence in random space [6] if the stochastic collocation method are based on one-dimensional Gauss–Hermite quadrature rules.

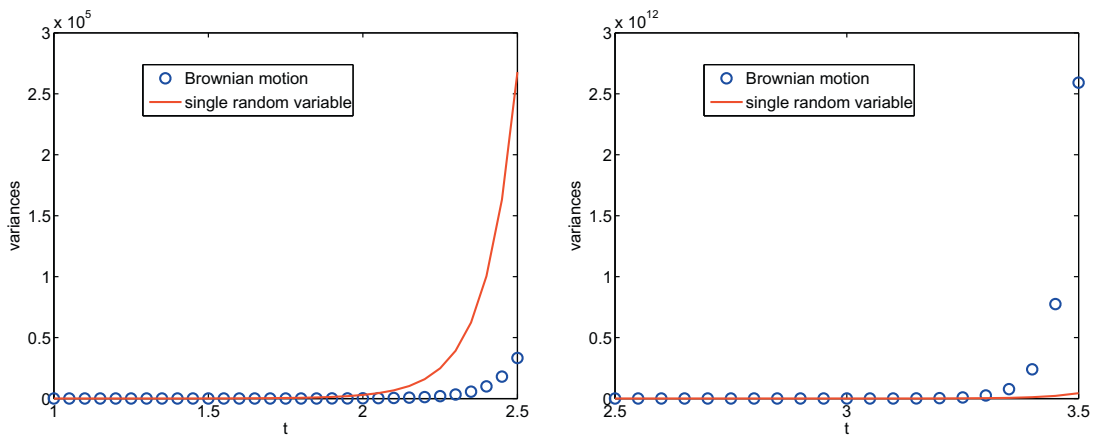
**Appendix B. A first-order model driven by different Gaussian processes**

Consider the following simple ordinary differential equation with multiplicative noise:

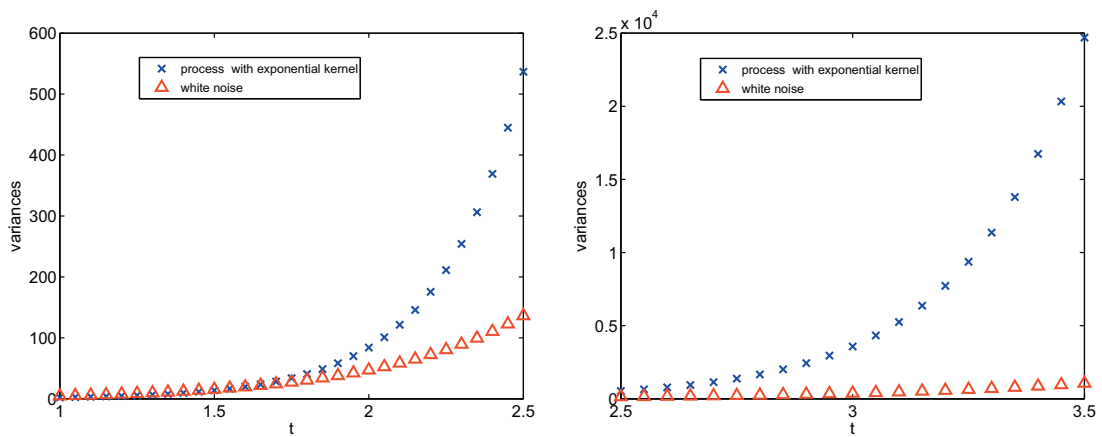
$$dy = k(t, \omega)ydt, \quad y(0) = y_0. \tag{B.1}$$



(a) Comparison between the cases of single random variable and a process with exponential kernel



(b) Comparison between the cases of Brownian motion and single random variable



(c) Comparison between the cases of white noise and a process with exponential kernel

**Fig. 8.** Comparison of variances of the solutions for four models of  $k(t)$  at large time:  $A = 1$ .

Here we take  $y_0 = 1$  for simplicity. Suppose  $k(t, \omega)$  is a Gaussian random variable or process with zero mean. Specifically,  $k(t, \omega)$  will take the following form:

- $k(t, \omega) =: \xi \sim \mathcal{N}(0, 1)$ .
- $k(t, \omega) =: V(t, \omega)$  where the two-point correlation function of  $V(t)$  is  $\exp(-\frac{|t_1 - t_2|}{A})$ .

- $k(t, \omega) =: W(t, \omega)$  is the standard Brownian motion:  $\mathbb{E}[W(t)W(s)] = \min(t, s)$ .
- $k(t, \omega) =: \dot{W}(t, \omega)$  is the white noise:  $\mathbb{E}[\dot{W}(t)\dot{W}(s)] = \delta(t - s)$ .

### B.1. Appendix

**Remark 1.** When  $k(t, \omega) =: \dot{W}(t, \omega)$ , Eq. (B.1) is understood in the Stratonovich sense:

$$dy = y \circ dW(t), \quad y(0) = y_0. \quad (\text{B.2})$$

The exact solution to Eq. (B.1) is  $y = y_0 \exp(K(t))$ , where  $K(t) = \int_0^t k(s) ds$  is again Gaussian with mean zero and variance  $\sigma^2$ . Then we have the moments of the solution  $y$ , for  $m = 1, 2, \dots$ ,  $\mathbb{E}[y^m(t)] = y_0^m \exp\left(\frac{m^2}{2} \sigma^2\right)$ , where  $\sigma^2 = t^2$ ,  $2At + 2A^2\left(\exp\left(-\frac{t}{A}\right) - 1\right)$ ,  $\frac{t^3}{3}$ ,  $t$  for the listed processes, respectively. Figs. 7 and 8 illustrate the different behavior of second-order moments with small time  $t \in [0, 1]$  and larger time  $t > 1$ . The amplitudes of variances are similar to those of variances of the shock location in Fig. 6, indicating three different behaviors in three different time intervals.

### References

- [1] G. Lin, C.H. Su, G.E. Karniadakis, The stochastic piston problem, Proc. Nat. Acad. Sci. USA 101 (45) (2004) 15840–15845 (electronic).
- [2] O.M. Knio, O.P. Le Maître, Uncertainty propagation in CFD using polynomial chaos decomposition, Fluid Dyn. Res. 38 (9) (2006) 616–640.
- [3] H.N. Najm, Uncertainty quantification and polynomial chaos techniques in computational fluid dynamics, Annu. Rev. Fluid Mech. 41 (2009) 35–52. Palo Alto, CA.
- [4] B. Ksandal, Stochastic differential equations, sixth ed., An Introduction with Applications, Universitext, Springer-Verlag, Berlin, 2003.
- [5] D.B. Xiu, G.E. Karniadakis, The Wiener-Askey polynomial chaos for stochastic differential equations, SIAM J. Sci. Comput. 24 (2) (2002) 619–644.
- [6] Z. Zhang, B. Rozovskii, G.E. Karniadakis, Stochastic collocation methods for stochastic differential equation driven by white noise, in preparation.
- [7] P.E. Kloeden, E. Platen, Numerical solution of stochastic differential equations, Applications of Mathematics, vol. 23, Springer-Verlag, Berlin, 1992 (New York).
- [8] I. Babuska, F. Nobile, R. Tempone, A stochastic collocation method for elliptic partial differential equations with random input data, SIAM J. Numer. Anal. 45 (3) (2007) 1005–1034.
- [9] M. Tatang, G. McRae, Direct Treatment of Uncertainty in Models of Reaction and Transport, Tech. rep., Department of Chemical Engineering MIT, 1994.
- [10] D.B. Xiu, J.S. Hesthaven, High-order collocation methods for differential equations with random inputs, SIAM J. Sci. Comput. 27 (3) (2005) 1118–1139.
- [11] H. Niederreiter, Random number generation and quasi-Monte Carlo methods, CBMS-NSF Regional Conference Series in Applied Mathematics, vol. 63, Society for Industrial and Applied Mathematics (SIAM), Philadelphia, PA, 1992.
- [12] I.H. Sloan, H. Woźniakowski, When are quasi-Monte Carlo algorithms efficient for high-dimensional integrals?, J. Complex. 14 (1) (1998) 1–33.
- [13] I.G. Graham, F.Y. Kuo, D. Nuyens, R. Scheichl, I.H. Sloan, Quasi-Monte Carlo methods for elliptic PDEs with random coefficients and applications, J. Comput. Phys. 230 (10) (2011) 3668–3694.
- [14] H.W. Liepmann, A. Roshko, Elements of Gasdynamics, Galtit Aeronautical Series, John Wiley & Sons Inc., New York, 1957.
- [15] H. Holden, N.H. Risebro, Conservation laws with a random source, Appl. Math. Optim. 36 (2) (1997) 229–241.
- [16] G.-S. Jiang, C.-W. Shu, Efficient implementation of weighted ENO schemes, J. Comput. Phys. 126 (1) (1996) 202–228.
- [17] A. Genz, B.D. Keister, Fully symmetric interpolatory rules for multiple integrals over infinite regions with Gaussian weight, J. Comput. Appl. Math. 71 (2) (1996) 299–309.
- [18] H.J. Sussmann, On the gap between deterministic and stochastic ordinary differential equations, Ann. Probab. 6 (1) (1978) 19–41.
- [19] E. Wong, M. Zakai, On the convergence of ordinary integrals to stochastic integrals, Ann. Math. Stat. 36 (1965) 1560–1564.
- [20] Z. Zhang, B. Rozovskii, M.V. Tretyakov, G.E. Karniadakis, A multistage Wiener chaos expansion method for stochastic advection–diffusion–reaction equations, SIAM J. Sci. Comput. 34 (2) (2012) A914–A936.
- [21] L. Kocis, W.J. Whiten, Computational investigations of low-discrepancy sequences, ACM Trans. Math. Softw. 23 (1997) 266–294.
- [22] J. Matoušek, On the I2-discrepancy for anchored boxes, J. Complex. 14 (1998) 527–556.
- [23] E. Wong, M. Zakai, On the relation between ordinary and stochastic differential equations, Int. J. Eng. Sci. 3 (1965) 213–229.